This is a repository copy of *The three-dimensional development of the shearing instability of convection* .

White Rose Research Online URL for this paper:
http://eprints.whiterose.ac.uk/981/

The three-dimensional development of the shearing instability of convection

P.C. Matthews

Department of Theoretical Mechanics, University of Nottingham,
University Park, Nottingham NG7 2RD, UK

A.M. Rucklidge, N.O. Weiss and M.R.E. Proctor
Department of Applied Mathematics and Theoretical Physics,
University of Cambridge, Cambridge CB3 9EW, UK

Two-dimensional convection can become unstable to a mean shear flow. In three dimensions, with periodic boundary conditions in the two horizontal directions, this instability can cause the alignment of convection rolls to alternate between the x and y axes. Rolls with their axes in the y-direction become unstable to a shear flow in the x-direction that tilts and suppresses the rolls, but this flow does not affect rolls whose axes are aligned with it. New rolls, orthogonal to the original rolls, can grow, until they in turn become unstable to the shear flow instability. This behaviour is illustrated both through numerical simulations and through low-order models, and the sequence of local and global bifurcations is determined.

The instability of two-dimensional convection rolls to a mean flow has been the subject of much recent study [1–4]. If a roll tilts over, horizontal momentum will be transported to the top and bottom of the layer in such a way as to enhance the original tilt, and a vertical shear across the layer may be spontaneously generated. This mechanism is purely hydrodynamic, so the instability is not restricted to convective flows but can occur in any periodic cellular flow [5]. These mean flows may be important in a variety of contexts, including the generation of zonal winds in planetary atmospheres [6] and plasma flows in tokamaks [2].

The shear flow instability of two-dimensional convection is now well understood, and has been observed in experiments [7] and numerical simulations [3,4,8]. Low-order models of the instability have played a central role in interpreting the complicated dynamics associated with the development of mean flows [1,8]. The instability is favoured when the convection cells are narrow and when the Prandtl number is small. As the Rayleigh number R is increased above its critical value R_C, convection rolls are formed, having mirror planes of symmetry separating counter-rotating rolls (cf. figure 1a, c). Beyond a second critical value, the symmetric state is unstable and asymmetric tilted convection occurs, with a steady shear flow (cf. figure 1b, d). There are subsequent bifurcations to time-dependence, and global bifurcations lead to complicated dynamics [3,8].

This letter considers the extension of these results to three-dimensional convection. In this situation, the dynamics rapidly becomes more complicated than in two dimensional convection, since a shear flow suppresses convective rolls with their axes perpendicular to the shear, but not rolls whose axes are aligned with the shear. Thus we expect to find oscillations: rolls are formed and tilt over since they are unstable to shear; the shear then suppresses the original rolls, but orthogonal rolls grow, and in turn are suppressed by the shear flow that they engender. Here we unravel the details of the transitions from rolls to this three-dimensional shearing oscillation by supplementing numerical simulations of the PDEs for three-dimensional convection with a study of the bifurcations in a low-order ODE model.

Details of the numerical procedure are given elsewhere [9]. Periodic boundary conditions are imposed in both horizontal directions x and y, while the upper and lower boundaries are stress-free with fixed temperature. The fluid is compressible, but only weakly stratified, and we have checked that similar behaviour is obtained using a Boussinesq code. The Prandtl number σ is fixed at 0.8, and the aspect ratio is unity, so that the computational domain is a cube. The controlling parameter is the Rayleigh number, proportional to the temperature difference imposed across the layer. The PDEs are solved numerically using a pseudospectral representation in the two horizontal directions (16×16 Fourier modes) and fourth-order finite differences in the vertical direction (25 grid points).

We have constructed a model by truncating the PDEs for Boussinesq convection (the minimal truncation results in 23 ODEs) and taking the limit of narrow rolls, which reduces the order to seven; details are given elsewhere [8,10]. The resulting model is:

$$\dot{\Psi}_{x11} = \mu\Psi_{x11} + \Psi_{x11}\theta_{02} - \Psi_{x01}\Psi_{x12} - \beta\Psi_{y11}^2\Psi_{x11},$$

$$\dot{\Psi}_{x12} = -\nu\Psi_{x12} + \Psi_{x11}\Psi_{x01},$$

$$\dot{\Psi}_{x01} = -\frac{\sigma}{4}\Psi_{x01} + \frac{3(1+\sigma)}{4\sigma}\Psi_{x11}\Psi_{x12},$$

$$\dot{\theta}_{02} = -\theta_{02} - \Psi_{x11}^2 - \Psi_{y11}^2, \tag{1}$$

$$\dot{\Psi}_{y11} = \mu\Psi_{y11} + \Psi_{y11}\theta_{02} - \Psi_{y01}\Psi_{y12} - \beta\Psi_{x11}^2\Psi_{y11},$$

$$\dot{\Psi}_{y12} = -\nu\Psi_{y12} + \Psi_{y11}\Psi_{y01},$$

$$\dot{\Psi}_{y01} = -\frac{\sigma}{4}\Psi_{y01} + \frac{3(1+\sigma)}{4\sigma}\Psi_{y11}\Psi_{y12}.$$

Here, μ is the bifurcation parameter proportional to $(R/R_C - 1)$, $\nu = (9\sigma/4(1+\sigma)) - \mu$ and β is a small positive parameter. The mode Ψ_{x11} in (1) represents the amplitude of rolls in the x-direction, Ψ_{x12} is the mode that causes these rolls to tilt and Ψ_{x01} is the mean shear flow. The modes Ψ_{y11}, Ψ_{y12} and Ψ_{y01} are defined similarly, but for rolls aligned in the y-direction; θ_{02} represents perturbations to the horizontally averaged temperature. Since we are considering narrow rolls, half as wide as they are tall, we may neglect the higher-order shear modes that would be important in wider boxes [11].

We do not expect quantitative agreement between the ODEs (1) and the full PDEs, but understanding the bifurcations in the ODE model, particularly the global bifurcations, has proved essential in interpreting the behaviour of the PDEs. Truncated models like (1) can provide reliable descriptions of PDE behaviour only when the amplitudes of the modes and the driving forces are small. We examine behaviour only up to $R = 1.80R_C$ in this letter, and find that the PDE behaviour can be interpreted in terms of the ODEs with $\mu \le 0.20$.

The ODEs (1) have a number of symmetries and associated invariant subspaces inherited from the original PDEs. As μ is increased, symmetries are broken in a sequence of bifurcations that is the same in the PDEs as in the ODEs. The resulting steady solutions are summarized in table I. The first bifurcation at $\mu = 0$ creates rolls and squares. Rolls are stable and may be aligned in the x-direction (xR) or the y-direction (yR) – see figure 1(a,c). Squares (Sq) are unstable and are a saddle point in (1), so trajectories that start near squares tend towards one of the roll solutions. The next bifurcation breaks the mirror symmetry of the rolls, so xR lose stability to tilted x-rolls (xTR), tilted either to the left or the right (figure 1b). So far the behaviour has been within the two-dimensional subspaces, but the next bifurcation breaks into three dimensions: xTR lose stability to cross-rolls with $\Psi_{y11} \ne 0$; we will refer to the resulting solution as x-tilted squares (xTSq). There are additional unstable steady solutions, diagonally tilted squares (DTSq).

As μ is increased further, the system becomes time-dependent. The xTSq undergo a Hopf bifurcation leading to oscillatory tilted squares (xOTSq), without breaking the remaining reflection symmetry. The phase portrait of this solution is shown in figure 2(a) for the ODEs and (d) for the PDEs. For higher μ, the system approaches a heteroclinic, or global, bifurcation: the orbit visits xR, then xTR, then Sq before returning to xR (figure 2b, e). Beyond this bifurcation, a structurally stable heteroclinic cycle exists, linking xR, xTR, yR and yTR (figure 2c, f). The bifurcation sequence is summarized in figure 3.

The heteroclinic cycle as it appears in the PDEs is shown in figure 1. Each connection that makes up the heteroclinic cycle is within an invariant subspace and connects an unstable steady solution to a steady solution

that is stable within that subspace. There are two types of connection: from rolls to tilted rolls, and from tilted rolls to untilted orthogonal rolls. The connection from x-rolls to tilted x-rolls is within the $\Psi_{y11} = \Psi_{y12} = \Psi_{y01} = 0$ invariant subspace (in which convection is purely two-dimensional); within this subspace, tilted x-rolls are stable. The connection from tilted x-rolls to y-rolls is within the $\Psi_{y12} = \Psi_{y01} = 0$ invariant subspace (in which convection is three-dimensional but does not break the y reflection symmetry); within this subspace, y-rolls are stable. The heteroclinic cycle has infinite period, but in numerical simulations, which are affected by round-off errors, the period of the cycle is finite and dependent on the numerical precision. In addition, the direction of the shear flow that destabilizes the rolls is determined by numerical noise.

Structurally stable heteroclinic cycles often occur in systems with symmetry [12]. The value $\sigma = 0.8$ was selected for the simulations discussed in this letter as it provides the simplest of many possible scenarios. For higher values of σ, a Hopf bifurcation within the two-dimensional subspaces can occur while the heteroclinic cycle is stable, leading to a more complicated connection that links fixed points (rolls) and periodic orbits (oscillatory tilted rolls), or even chaotic attractors. For smaller σ, the xOTSq in the ODEs can undergo a period-doubling cascade before the heteroclinic cycle is formed, just as in the PDEs. A detailed discussion of the dependence of the behaviour of the PDEs on σ is beyond the scope of this letter; this will be undertaken in a future work.

In summary, we have shown how the instability of convection to a mean shear flow can lead to three-dimensional behaviour via a series of local and global bifurcations. The ODE model has proved to be essential for the interpretation of complicated dynamics of three-dimensional convection.

ACKNOWLEDGEMENTS

[1] L. N. Howard and R. Krishnamurti, "Large-scale flow in turbulent convection: a mathematical model," J. Fluid Mech. **170**, 385 (1986).

[2] J. M. Finn, J. F. Drake and P. N. Guzdar, "Instability of fluid vortices and generation of sheared flow," Phys. Fluids B **4**, 2758 (1992).

[3] P. C. Matthews, M. R. E. Proctor, A. M. Rucklidge and N. O. Weiss, "Pulsating waves in nonlinear magnetoconvection," Physics Letters A **183**, 69 (1993).

[4] J. Prat, J. M. Massaguer and I. Mercader, "Large-scale flows and resonances in 2-D thermal convection," Phys. Fluids **7**, 121 (1995).

[5] P. Tabeling, O. Cardoso and B. Perrin, "Chaos in a linear array of vortices," J. Fluid Mech. **213**, 511 (1990).

[6] F. H. Busse, "Generation of mean flows by thermal convection," Physica **9D**, 287 (1983).

[7] R. Krishnamurti and L. N. Howard, "Large-scale flow generation in turbulent convection," Proc. Nat. Acad. Sci. U.S.A. **78**, 1981 (1981).

[8] A. M. Rucklidge and P. C. Matthews, "Analysis of the shearing instability in nonlinear convection and magnetoconvection," Nonlinearity, submitted (1996).

[9] P. C. Matthews, M. R. E. Proctor and N. O. Weiss, "Compressible magnetoconvection in three dimensions: planforms and nonlinear behaviour," J. Fluid Mech. **305**, 281 (1995).

[10] A. M. Rucklidge and P. C. Matthews, "The shearing instability in magnetoconvection," in *Double-Diffusive Convection*, edited by A. Brandt and H. J. S. Fernando (AGU, Washington, 1995).

[11] K. B. Hermiz, P. N. Guzdar and J. M. Finn, "Improved low-order model for shear flow driven by Rayleigh–Bénard convection," Phys. Rev. E **51**, 325 (1995).

[12] M. Krupa, "Robust heteroclinic cycles," preprint (1995).

Symbol	Name	Defining equations
xR	x-rolls	$\Psi_{x12} = \Psi_{x01} = 0$
		$\Psi_{y11} = \Psi_{y12} = \Psi_{y01} = 0$
Sq	squares	$\Psi_{x11} = \pm\Psi_{y11}$
		$\Psi_{x12} = \Psi_{x01} = 0$
		$\Psi_{y12} = \Psi_{y01} = 0$
xTR	tilted x-rolls	$\Psi_{y11} = \Psi_{y12} = \Psi_{y01} = 0$
xTSq	x-tilted squares	$\Psi_{y12} = \Psi_{y01} = 0$
DTSq	diagonally tilted squares	$\Psi_{x11} = \pm\Psi_{y11}$
		$\Psi_{x01} = \pm\Psi_{y01}$

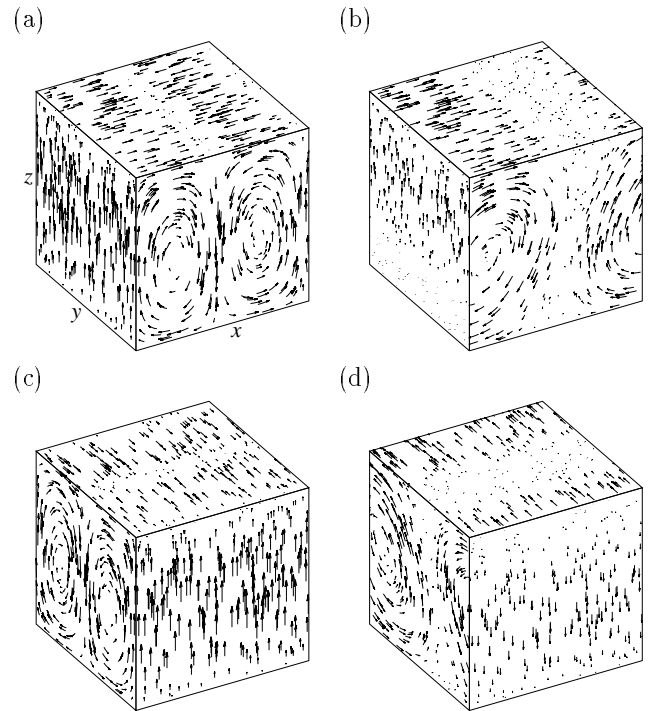TABLE I. Steady solutions of the PDEs and ODEs (1).

FIG. 1. Steady solutions of the PDEs. (a) x-rolls (xR), invariant under reflections in the vertical plane that lies between the pair of rolls. (b) tilted x-rolls (xTR): the mirror symmetry is broken and there is a spontaneously generated shear flow across the layer. (c) y-rolls (yR), orthogonal to x-rolls. (d) tilted y-rolls (yTR). These steady solutions of the PDEs are all unstable and there is a structurally stable heteroclinic cycle between them: x-rolls are unstable to shear, leading to tilted x-rolls; these are unstable to cross-rolls, leading to y-rolls, which in turn give way to tilted y-rolls, and then back to x-rolls. The Rayleigh number is $R = 1.80R_C$. Velocity arrows are projected onto the sides of the cube.
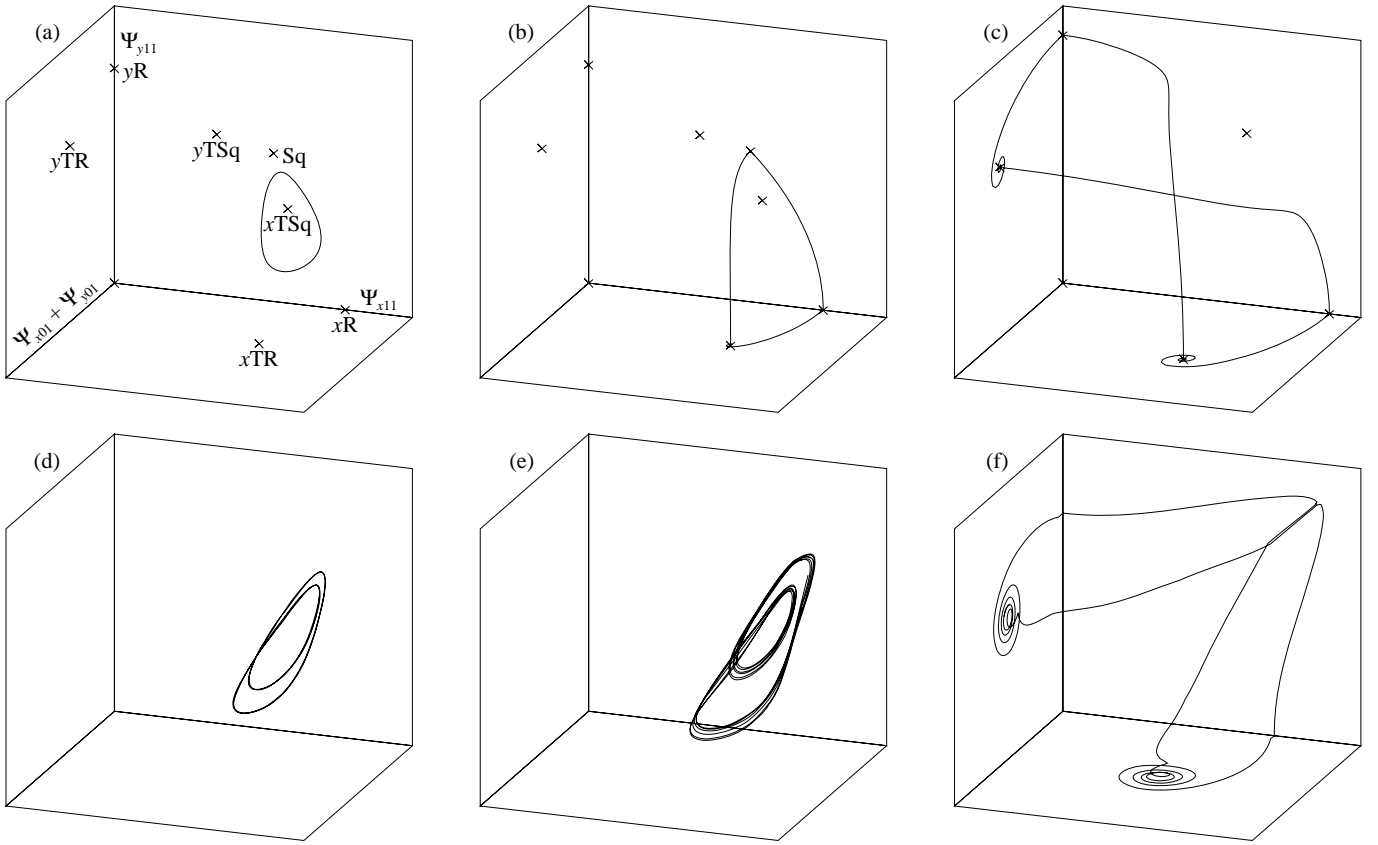
FIG. 2. Unsteady solutions of the ODEs (1) (with $\sigma = 0.8$ and $\beta = 0.1$) in (a)–(c) and the PDEs in (d)–(f). The xTSq have lost stability to form xOTSq (a: $\mu = 0.15$); this undergoes a heteroclinic bifurcation (b: $\mu \approx 0.154945$) when it collides with xR, xTR and Sq. The structurally stable heteroclinic cycle (c: $\mu = 0.20$) visits xR, xTR, yR and yTR before returning to xR. A similar sequence is seen in the PDEs: the xOTSq (d: $R = 1.60R_C$) become chaotic as they approach the heteroclinic bifurcation with squares (e: $R = 1.65R_C$) to form the heteroclinic cycle (f: $R = 1.80R_C$). The fixed points that make up the cycle are illustrated in figure 1.
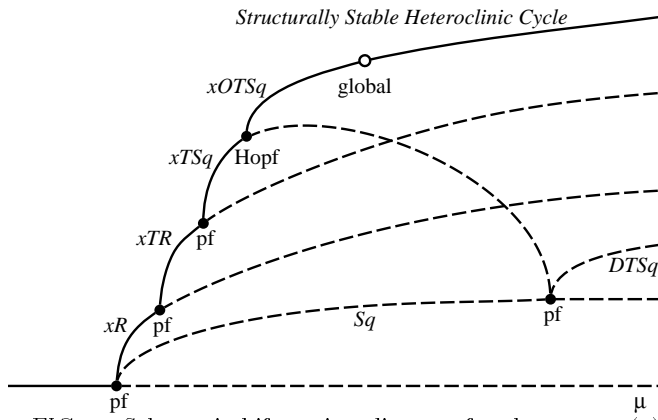
4

FIG. 3. Schematic bifurcation diagram for the system (1) and the PDEs. Closed circles represent local (pitchfork and Hopf) bifurcations, and the open circle represents the global (heteroclinic) bifurcation.